![The University of Osaka Institutional Knowledge Archive - OUKA logo]

The University of Osaka
Institutional Knowledge Archive

Title	Solution properties of amylose tris(3,5-dimethylphenylcarbamate) and amylose tris(phenylcarbamate): Side group and solvent dependent chain stiffness in methyl acetate, 2-butanone, and 4-methyl-2-pentanone
Author(s)	Tsuda, Maiko; Terao, Ken; Nakamura, Yasuko et al.
Citation	Macromolecules. 2010, 43(13), p. 5779-5784
Version Type	AM
URL	https://hdl.handle.net/11094/81829
rights	This document is the Accepted Manuscript version of a Published Work that appeared in final form in Macromolecules, © American Chemical Society after peer review and technical editing by the publisher. To access the final edited and published work see https://doi.org/10.1021/ma1006528.
Note	

The University of Osaka Institutional Knowledge Archive : OUKA

https://ir.library.osaka-u.ac.jp/

The University of Osaka

Solution Properties of Amylose Tris(3,5-dimethylphenylcarbamate) and Amylose Tris(phenylcarbamate): Side Group and Solvent Dependent Chain Stiffness in Methyl Acetate, 2-Butanone, and 4-Methyl-2-pentanone

Maiko Tsuda,[†] Ken Terao,[,†] Yasuko Nakamura,[†] Yusuke Kita,[†] Shinichi Kitamura,[‡] and Takahiro Sato[†]*

[†]Department of Macromolecular Science, Graduate School of Science, Osaka University, 1-1, Machikaneyama-cho, Toyonaka, Osaka 560-0043, Japan, and [‡]Graduate School of Life and Environmental Sciences, Osaka Prefecture University, Gakuen-cho, Nakaku, Sakai, Osaka 599-8531, Japan

* Corresponding author. E-mail: kterao@chem.sci.osaka-u.ac.jp

ABSTRACT: Five amylose tris(3,5-dimethylphenylcarbamate) (ADMPC) samples ranging in weight-average molecular weight M_w from 1.7×10^4 to 3.4×10^5 were studied by light and small-angle X-ray scattering, sedimentation equilibrium, and viscometry in methyl acetate (MEA), 2-butanone (MEK), and 4-methyl-2-pentanone (MIBK) at 25 °C. Seven amylose tris(phenylcarbamate) (ATPC) samples whose M_w ranges between 2×10^4 and 3×10^6 were also investigated in MEK at 25 °C. The radii of gyration, particle scattering functions, and intrinsic viscosities determined as a function of M_w were analyzed in terms the cylindrical wormlike chain model mainly to determine the Kuhn segment length λ^{-1} and the contour length h (or the helix pitch) per residue. While the obtained h values (0.36 – 0.38 nm) of ADMPC are quite insensitive to the solvents, the λ^{-1} value is not only 1.5 – 3 times larger than that of ATPC in the corresponding solvent, but also significantly increases with an increase of the molar volume of the solvent and it reaches 73 nm in MIBK, which is the highest value for previously investigated phenylcarbamate derivatives of polysaccharides. This high stiffness is most likely due to the steric hindrance of the solvent molecules H-bonding with the NH groups of the polymer.

Introduction

Polysaccharide phenylcarbamates, which are widely used as a chiral stationary phase,[1] have nanosized cavity-like structures around their NH and C=O groups.[2,3] Some recent studies[2,3,4,5,6] focused on the local conformation of amylose tris(3,5-dimethylphenylcarbamate) (ADMPC, Chart 1). Wenslow and Wang[4] inferred from their solid-state NMR spectra that ADMPC has a helix with a number of folds less than six. Furthermore, Yamamoto et al.[2] proposed a left-handed fourfold helical conformation from molecular modeling with the aid of 2D-NOESY NMR measurements in CDCl3. Further, its local conformational change with an addition of polar solvents was detected by infrared absorption (IR), X-ray diffraction, and solid-state NMR.[3,5] More significant difference was observed in the vibrational circular dichroism spectra in the presence of various alcohols.[6] In spite of such interest, we found no reports for the global conformation of ADMPC in solution while it was reported that amylose tris(phenylcarbamate) (ATPC) molecules behave as semiflexible chains in solution,[7] and furthermore, its unperturbed dimensions significantly depend on the solvent.[7a]

Very recently, we analyzed dimensional and hydrodynamic properties of ATPC in three solvents having a carbonyl group (esters and a ketone) in terms of the wormlike chain[8] and found that both the helix pitch (or contour length) h per residue and the Kuhn segment length λ^{-1} (or more generally, the stiffness parameter of the helical wormlike chain[9,10]) measurably increase with increasing the molar volume v_M of the solvent.[11] We thus inferred that solvent molecules wedge into the domain sandwiched between the neighboring phenylcarbamate groups and consequently the main chain of ATPC extends

1

and stiffens. On the other hand, such chain extension and stiffening were not observed for amylose tris(n-butylcarbamate) in various alcohols having different v_M,[12] indicating that the solvent dependence of the main chain conformation has something to do with the side-group bulkiness. This also prompted us to investigate dimensional and hydrodynamic properties of ADMPC, which has bulkier side groups than that of ATPC.

The first aim of this study is thus to identify whether the larger side groups on ADMPC stiffen and/or extend the main chain; in the case of cellulosic chains, dimensional and hydrodynamic properties of cellulose tris(3,5-dimethylphenylcarbamate) (CDMPC) do not measurably differ from those of cellulose tris(phenylcarbamate) (CTPC).[13] The second is to investigate solvent effects to the chain stiffening and extension of ADMPC owing to the steric hindrance of H-bonding solvent molecules. We therefore studied solution properties of ADMPC to determine their wormlike-chain parameters (h and λ^{-1}) in 4-methyl-2-pentanone (MIBK), 2-butanone (MEK), and methyl acetate (MEA). The parameters were also determined for ATPC in MEK to compare them with those for ADMPC in the same solvent; it should be noted that the corresponding analysis for ATPC in MEA and MIBK has been reported in our recent paper.[11]
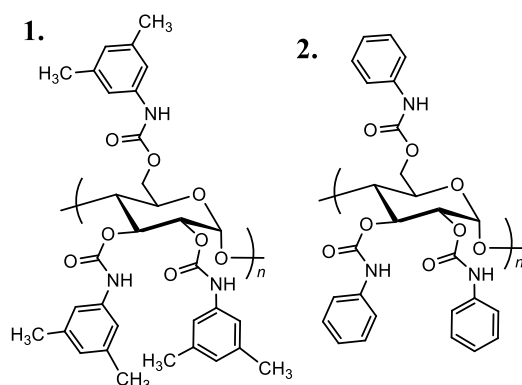

Chart 1. Chemical structures of ADMPC (1) and ATPC (2).

Experimental Section

Materials. Five ADMPC samples were prepared from enzymatically synthesized amylose samples, which have no branching and narrow molecular weight distribution,[14,15] in the manner reported by Okamoto et al.[2,16] The ratios of the weight- to number-average molecular weight M_w/M_n for the resultant samples were estimated to be ~ 1.1 from size-exclusion chromatography using dimethylformamide (DMF) as an eluent. Each sample was further purified by successive fractional precipitation with DMF or MEK as a solvent and methanol as a precipitant. Appropriate middle fractions were designated as ADMPC17K, ADMPC25K, ADMPC49K, ADMPC160K, and ADMPC340K.

The degree of substitution DS for the five ADMPC samples was estimated to be nearly three (2.9 – 3.2) from the mass ratio of nitrogen to carbon determined by elemental analysis. Substantially equivalent DS was obtained from ^{1}H NMR spectra (JEOL GSX400-NMR) for the samples ADMPC17K and ADMPC25K in CDCl$_3$ at 30 °C.

Seven previously investigated ATPC samples[17] (ATPC3M, ATPC800K, ATPC500K, ATPC300K, ATPC200K, ATPC50K, and ATPC20K) ranging in the weight-average molecular weight M_w from 2×10^4 to 3×10^6 were also used for this study. The ratios of z-average molecular weight (M_z) to M_w or M_w / M_n were determined between 1.05 and 1.11.

MIBK, MEK, and MEA used for the following measurements were purified by fractional distillation over CaH$_2$.

Light Scattering. Static light scattering (SLS) measurements were made for ADMPC340K, ADMPC160K, and ADMPC25K in MIBK, MEK, and MEA, and ADMPC49K, ATPC3M, ATPC800K, ATPC500K, ATPC300K, and ATPC200K in MEK all at 25 °C on a Fica-50 light scattering photometer with vertically polarized incident light of 436-nm wavelength. Procedures including optically clean and calibration of the photometer were recently described.[17] Scattering measurements were also made for the depolarized components because optical anisotropic effects were appreciable for ADMPC25K and

ADMPC49K in solution while they were negligible for ATPC in MEK. It should be noted that the effect is also appreciable for CDMPC in 1-methyl-2-pyrrolidone (NMP)[18,19] while that for CTPC is negligible.[20] The reduced scattering intensities $R_{\theta,\text{Hv}}$ and $R_{\theta,\text{Uv}}$ for vertically polarized incident light were determined with or without analyzer in the horizontal direction, respectively, at scattering angle θ. The obtained data were analyzed according to the following equations[21,22,23] to determine M_w, the second virial coefficient A_2, the optical anisotropy factor δ, and an apparent radius of gyration $<S^2>^*$, which is different from the z-average mean-square radius of gyration $<S^2>_\text{z}$ for semiflexible chains unless $\delta = 0$.

$$\lim_{c \to 0} \left(\frac{Kc}{R_{\theta,\text{Uv}}} \right)^{1/2} = M_{\text{w,app}}^{-1/2} P(k)_{\text{app}}^{-1/2} = M_{\text{w,app}}^{-1/2} \left[1 + \frac{1}{6} \left\langle S^2 \right\rangle_{\text{z,app}}^{1/2} k^2 + ... \right]$$

(1)

$$\lim_{\theta \to 0} \left(\frac{Kc}{R_{\theta,\text{Uv}}} \right)^{1/2} = \left(\frac{Kc}{R_{0,\text{Uv}}} \right)^{1/2} = M_{\text{w,app}}^{-1/2} \left[1 + A_{2,\text{app}} M_{\text{w,app}} c + ... \right]$$

(2)

$$\lim_{c \to 0} \frac{R_{0,\text{Hv}}}{R_{0,\text{Uv}}} = \frac{3\delta}{1 + 7\delta}$$

(3)

where

$$M_{\text{w,app}} = (1 + 7\delta) M_\text{w}$$

(4)

$$\left\langle S^2 \right\rangle_{\text{z,app}} = (1 + 7\delta)^{-1} \left\langle S^2 \right\rangle^*$$

(5)

$$A_{2,\text{app}} = (1 + 7\delta)^{-2} A_2$$

(6)

Here, K, k, c, and $P(k)_{\text{app}}$ are the optical constant, the absolute value of the scattering vector, the polymer mass concentration, and the apparent scattering function, respectively.

The specific refractive index increments $\partial n/\partial c$ at wavelength $\lambda_0 = 436$ nm were determined at 25 °C to be 0.186 cm^{3}g^{-1}, 0.201 cm^{3}g^{-1}, and 0.214 cm^{3}g^{-1} for ADMPC160K in MIBK, MEK, MEA, respectively, and 0.202 cm^{3}g^{-1} for ATPC800K in MEK.

Small-Angle X-ray Scattering. SAXS measurements were made with an imaging plate detector at the BL40B2 beamline in SPring-8 for ADMPC17K, ADMPC25K, and ADMPC49K in MIBK, MEK, and MEA, and ATPC20K and ATPC50K in MEK, all at 25 °C (see ref 17 for experimental details). The excess scattering intensities obtained for four solutions with different c were analyzed using the Berry square-root plot[21] to determine the particle scattering function $P(k)$ and $<S^2>_\text{z}$.

Ultracentrifugation. Sedimentation equilibrium measurements were made for ADMPC17K in MEK at 25 °C on a Beckman Optima XL-I ultracentrifuge at a rotor speed of 19,000 rpm to determine M_w, A_2, and M_z/M_w (See refs [17,24] for experimental details and data analysis). The concentration profile in each double sector cell was determined from the Rayleigh interference pattern at $\lambda_0 = 675$ nm. The $\partial n/\partial c$ value at this λ_0 was estimated to be 0.185 cm^{3}g^{-1} with the aid of $\partial n/\partial c$ plotted against λ_0^{-2} (see Supporting Information). The partial specific volume $\bar{v}$ of ADMPC17K in MEK at 25 °C was determined to be 0.768 cm^{3}g^{-1} using an Anton Paar DMA5000 densitometer.

Viscometry. Viscosity measurements for the five ADMPC samples in MIBK, MEK, and MEA, and the seven ATPC samples in MEK at 25 °C were made using a four-bulb low-shear capillary viscometer and conventional capillary viscometers of Ubbelohde type to determine the intrinsic viscosity $[\eta]$; the shear-rate effect on $[\eta]$ was insignificant even for ATPC3M. The difference between the solution and solvent densities were taken into account in evaluation of relative viscosity; $\bar{v}$ values to calculate solution density were determined at 25 °C to be 0.772 cm^{3}g^{-1} and 0.767 cm^{3}g^{-1} for ADMPC160K in MIBK and MEA, respectively. The obtained Huggins constant for ADMPC was 0.40 – 0.52 for the highest M_w sample (ADMPC340K) and 0.79 (in MIBK) – 1.1 (in MEA) for the lowest (ADMPC17K); they tend to increase with decreasing M_w.

Infrared Absorption (IR). IR spectra for ADMPC17K in MEA, MEK, and MIBK at 25°C were determined using an FT/IR 4200 (JASCO) with a solution cell made of CaF_2 (0.05 mm path length). Concentrations of test solutions were set to be ~ 0.01 g cm^{-3}.

Results

Each concentration dependence of $(Kc/R_{0,\mathrm{Uv}})^{1/2}$ (see Supporting Information) had a positive slope, indicating positive A_2 and hence MIBK, MEK, and MEA are good solvents for ADMPC. Numerical M_w and A_2 values were obtained by means of eqs 4 and 6. The δ value was at most 9.4×10^{-3}, and hence the contribution to M_w for the current samples was less than 7 %. The M_w values evaluated in the three solvents were in agreement within ±3%. The average M_w values are summarized in Table 1 along with A_2 in each solvent. This table includes the M_w and A_2 values determined from sedimentation equilibrium for ADMPC17K; its M_z/M_w was estimated to be 1.03. The A_2 values for the five ATPC samples (ATPC3M, …, ATPC200K) in MEK were obtained to be in a range between 1.9 and 2.3 $\times 10^{-4}$ mol cm^{3}g^{-2}, showing that MEK is a good solvent for ATPC, while their M_w values are consistent with those determined previously in the other solvents.[11,17] Both $<S^2>_{z,\mathrm{app}}$ (SLS) and $<S^2>_z$ (SAXS) were obtained from the initial slope of the Berry plots[21] (Figure 1); the latter values are presented in Table 1.
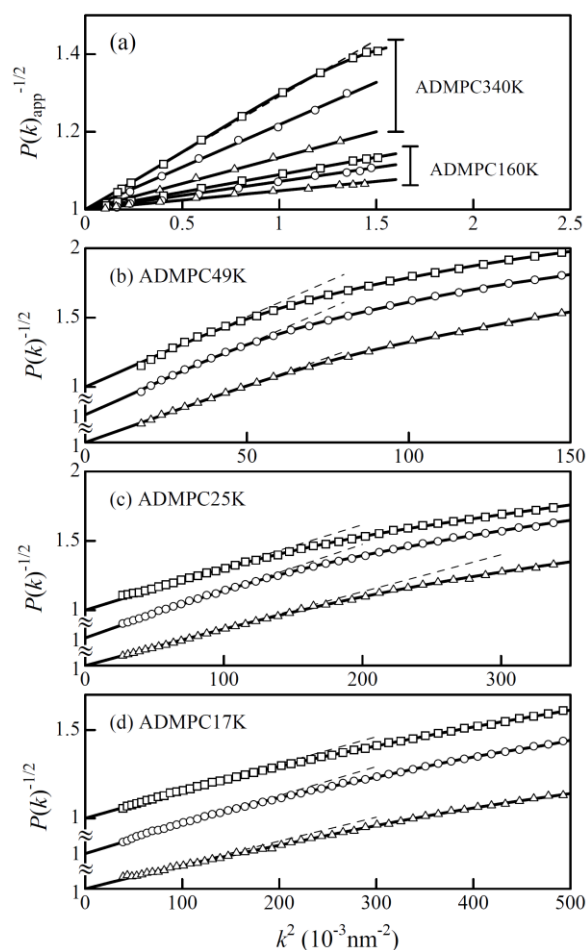

Figure 1. Angular dependence of $P(k)_{\mathrm{app}}^{-1/2}$ (from SLS) or $P(k)^{-1/2}$ (from SAXS) for indicated ADMPC samples in MIBK (squares), MEK (circles), and MEA (triangles) at 25 °C.

Table 1. Molecular Characteristics and Physical Properties of ADMPC Samples in 4-Methyl-2-pentanone (MIBK), 2-Butanone (MEK), and Methyl Acetate (MEA) at 25 °C

Sample	$M_w/10^3$	in MIBK			in MEK			in MEA		
		A_2 [d]	$<S^2>_z^{1/2}$ [e]	$[\eta]$ [f]	A_2 [d]	$<S^2>_z^{1/2}$ [e]	$[\eta]$ [f]	A_2 [d]	$<S^2>_z^{1/2}$ [e]	$[\eta]$ [f]
ADMPC340K	341 [a]	2.7 [a]	42.0 [a]	239	1.5 [a]	36.4 [a]	180	1.3 [a]	28.4 [a]	98.3
ADMPC160K	163 [a]	2.4 [a]	23.3 [a]	119	1.9 [a]	20.9 [a]	93.4	0.9 [a]	17.2 [a]	58.7
ADMPC49K	48.8 [a]		7.8 [b]	27.9	4 [a]	7.8 [b]	25.0		7.0 [b]	21.3
ADMPC25K	25.4 [a]	3 [a]	4.3 [b]	12.8	6 [a]	4.5 [b]	11.5	3 [a]	4.0 [b]	10.7
ADMPC17K	16.9 [c]		3.0 [b]	7.81	6.5 [c]	3.1 [b]	7.02		2.9 [b]	6.61

[a] SLS. [b] SAXS. [c] Sedimentation equilibrium. [d] In units of 10^{-4} mol cm^{3}g^{-2}. [e] In units of nm. [f] In units of cm^{3}g^{-1}.

Figure 2 illustrates $[\eta]M_0$ plotted against M_w/M_0 for ADMPC and ATPC in MIBK, MEK, and MEA at 25 °C where M_0 denotes the molar mass of the repeat unit (M_0 = 603.7 for ADMPC and 519.5 for ATPC). In each solvent, the $[\eta]$ data for ADMPC have larger slope than that for ATPC, suggesting that the higher chain rigidity of the former. A further important point is that the slope of ADMPC significantly increases in the order of MEA < MEK < MIBK, showing that the main chain stiffness increases with this order.
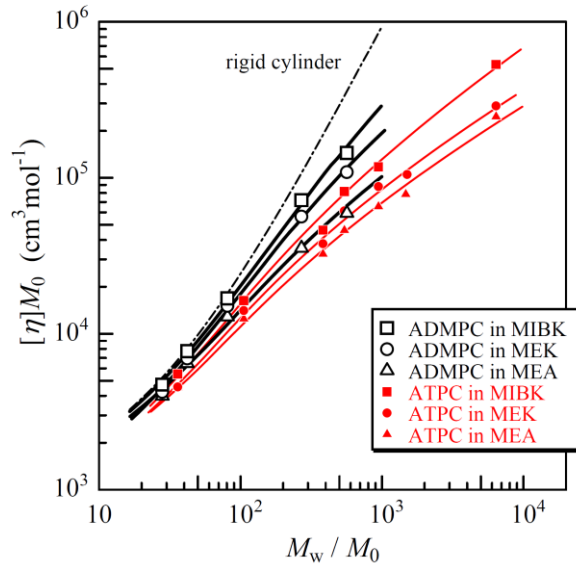

Figure 2. Molecular weight dependence of $[\eta]M_0$ for ADMPC in MIBK (open squares), MEK (open circles), MEA (open triangles) and for ATPC (filled circles) in MEK along with our previous data [11] for ATPC in MIBK (filled squares) and MEA (filled triangles), all at 25 °C. Solid curves, theoretical values for the wormlike cylinder model with the parameters listed in Table 2; a dot-dashed curve, theoretical values in the rod limit (h = 0.355 nm and d = 2.6 nm). See ref [11] for the wormlike chain parameters of ATPC in MIBK and MEA.

This conformational difference is also recognizable in the scattering function. The Holtzer plot[25] for ADMPC49K in MIBK (Figure 3) has a plateau (k = 0.1 – 0.5 nm^{-1}), showing high rigidity of ADMPC in the solvent. On the one hand, that in MEA has an appreciable peak at $k \sim 0.2$ nm^{-1}, indicating that the main chain of ADMPC is more flexible in MEA than in the other solvents.
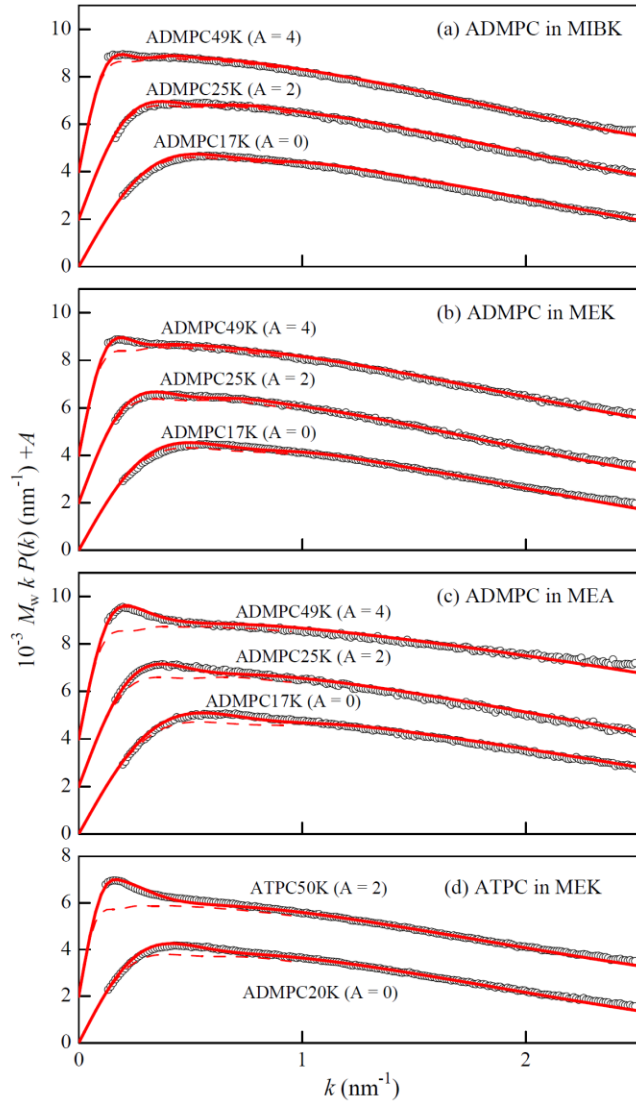
Figure 3. Reduced Holtzer plots for indicated ADMPC samples in MIBK, MEK, and MEA at 25 °C and ATPC samples in MEK at 25 °C. Circles, experimental data. Solid curves, theoretical values for the unperturbed wormlike cylinders with the parameters listed in Table 2. Dashed lines, theoretical values in the rod limit ($\lambda = 0$).

Discussion

Wormlike Chain Analysis. *Scattering Function.* The above mentioned Holtzer plots were analyzed in terms of the Nakamura and Norisuye theory[26] for unperturbed cylindrical wormlike chains, which is characterized by λ^{-1}, the contour length L, and the chain diameter d. The parameter L is related to the molecular weight M by $L = M/M_L$, with M_L being the molar mass per unit contour length. The two parameters, M_L and d, were determined unequivocally by a curve fitting method since the theoretical $P(k)$ is substantially the same as that for the rigid cylinder except for the low-k range.[26] Indeed, the theoretical dashed curves (mostly hidden behind the corresponding solid curves) calculated for the rigid cylinders with M_L and d listed in Table 2 reproduce quantitatively the experimental $P(k)$ in the k range between 0.8 nm^{-1} and 2.5 nm^{-1}. The rest parameter λ^{-1} was determined to be 20 ± 3 nm and 18 ± 2 nm for ADMPC in MEA and ATPC in MEK, respectively, since the dashed curves for these systems deviate appreciably from the experimental data in the range of $k < 0.8$ nm^{-1}. On the other hand, only a slight discrepancy between the data points and the corresponding dashed curve is however seen for ADMPC in MIBK and MEK, indicating their λ^{-1}'s are considerably higher than 20 nm. In fact, the theoretical solid curves for the wormlike cylinder with λ^{-1} determined from [η] (70 nm for ADMPC in MIBK and 38 nm in MEK, see below) excellently trace the experimental $P(k)$.

Intrinsic Viscosity. The Yamakawa-Fujii-Yoshizaki theory[9,27,28] for the intrinsic viscosity of an unperturbed wormlike cylinder was used to analyze our [η] data for ADMPC and ATPC. The excluded-volume effects were taken into account by use of the combination of the Barrett function[29] and the quasi-two-parameter (QTP) theory.[9,30,31] The theoretical intrinsic viscosity for the perturbed

6

wormlike cylinder can be calculated with the four parameters, M_L, λ^{-1}, d, and the excluded volume strength B. By curve fitting, the two parameters λ^{-1} and d were determined using M_L obtained from $P(k)$ because all the parameters cannot uniquely be estimated from our experimental $[\eta]$ data. The excluded-volume effects were found to be negligible in the M_w range studied; hence the last parameter B was not estimated. While the obtained λ^{-1} values for ADMPC in MEA and ATPC in MEK are substantially the same as those from $P(k)$, the d value estimated from $[\eta]$ is quite larger than the above mentioned values from $P(k)$ in each system (see Table 2). This is well-known tendency not only for amylose carbamates[11,17] but also for other flexible[9] and stiff[32] polymers, because the d value determined from $P(k)$ reflects the distributions of electrons as the scatterers around the chain contour.

Table 2. Wormlike Chain Parameters for ADMPC and ATPC at 25 °C

Method	M_L (nm^{-1})	λ^{-1} (nm)	d (nm)
ADMPC in MIBK			
$P(k)$	1700 ± 50	70 [a]	1.6 ± 0.1
$[\eta]$	1700 [a]	70 ± 5	2.6
$<S^2>_z$	1630 ± 50	75 ± 5	–
ADMPC in MEK			
$P(k)$	1580 ± 50	38 [a]	1.7 ± 0.1
$[\eta]$	1580 [a]	38 ± 3	2.1
$<S^2>_z$	1550 ± 50	43 ± 3	–
ADMPC in MEA			
$P(k)$	1660 ± 50	20 ± 3	1.3 ± 0.1
$[\eta]$	1660 [a]	20 ± 2	2.5
$<S^2>_z$	1650 ± 50	25 ± 2	–
ATPC in MEA			
$P(k)$	1350 ± 30	18 ± 2	1.7 ± 0.1
$[\eta]$	1350 [a]	16 ± 2	2.0
$<S^2>_z$	1300 ± 50	19 ± 2	–

[a] Assumed values.

Optical Anisotropy Factor and Radius of Gyration. If the ADMPC chain can be modeled by the wormlike chain with cylindrically symmetric polarizabilities, Nagai's expression[23] for $<S^2>*$ is written in a good approximation as[33]

$$\left\langle S^2\right\rangle* = \left\langle S^2\right\rangle - f_{Uv} \tag{7}$$

with

$$f_{Uv} = \frac{1}{45\lambda^2}\left[\varepsilon\left(1 - \frac{4}{3\lambda L} + \frac{13}{18(\lambda L)^2}\right) - \frac{23\varepsilon^2}{252\lambda L}\left(1 - \frac{103}{138\lambda L}\right)\right] \quad (\lambda L \geq 2) \tag{8}$$

where ε is the polarizability parameter defined by $\varepsilon = 3(\alpha_1 - \alpha_2)/(\alpha_1 + 2\alpha_2)$. Here, α_1 and α_2 are the longitudinal and transverse polarizabilities per unit contour length of the chain. The factor ε is related to δ by[23]

$$\delta = \frac{\varepsilon^2}{135\lambda L}\left\{1 - \frac{1}{6\lambda L}[1 - \exp(-6\lambda L)]\right\} \tag{9}$$

Molecular weight dependence of δ illustrated in Figure 4 are well fitted by the theoretical curves calculated using the λ^{-1} and M_L values determined from $P(k)$ and $[\eta]$ (Table 2), and the following $|\varepsilon| = 0.52$, 0.68, 1.2 for ADMPC in MIBK, MEK, MEA, respectively; these values are smaller than those for CDMPC in NMP ($|\varepsilon| = 2.8$).[19] The f_{Uv} values calculated from eq 8 are only $0.7 - 1\%$ and $1.2 - 2.2\%$ of the corresponding $<S^2>^*$ for ADMPC340K and ADMPC160K, respectively, and therefore the difference in $<S^2>^*$ and $<S^2>_z$ for our ADMPC samples is mostly negligible.
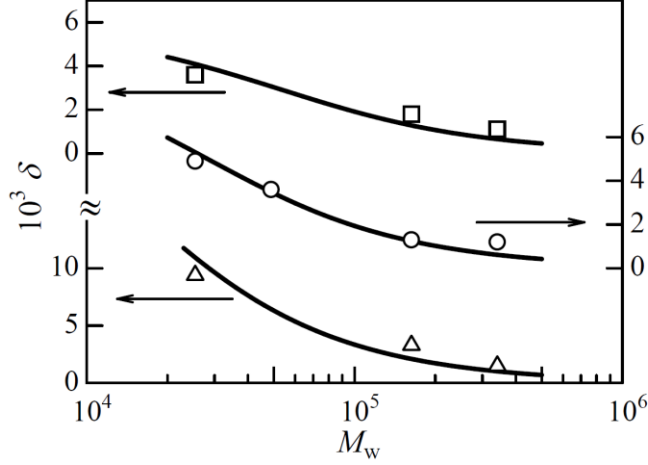
Figure 4. Molecular weight dependence of the optical anisotropy factor δ for ADMPC in MIBK (squares), MEK (circles), and MEA (triangles) at 25 °C. The curve represents the theoretical values calculated from eq 9 (see text for the parameters).

The obtained $<S^2>_z$ data for ADMPC and ATPC were analyzed by means of the unperturbed wormlike chain, whose mean-square radius of gyration $<S^2>$ is expressed as[34]

$$\left\langle S^2 \right\rangle = \frac{L}{6\lambda} - \frac{1}{4\lambda^2} + \frac{1}{4\lambda^3 L} - \frac{1}{8\lambda^4 L^2}\left[1 - \exp(-2\lambda L)\right]$$

(10)

since the intramolecular excluded-volume effects on $[\eta]$ are negligible. The contribution of the chain thickness to $<S^2>^{1/2}$ is also negligible ($< 1.8\%$) even for ADMPC17K and ATPC20K when the effect is considered as the addition of $d^2/8$ to the right-hand side of the equation[35] with the d value determined from $P(k)$. The theoretical values calculated with the parameters in Table 2 excellently fit the corresponding experimental data as shown in Figure 5. The obtained M_L and λ^{-1} are consistent with those from $P(k)$ and $[\eta]$, concluding that the accurate wormlike chain parameters were determined for ADMPC in the three solvents and ATPC in MEK at 25 °C.
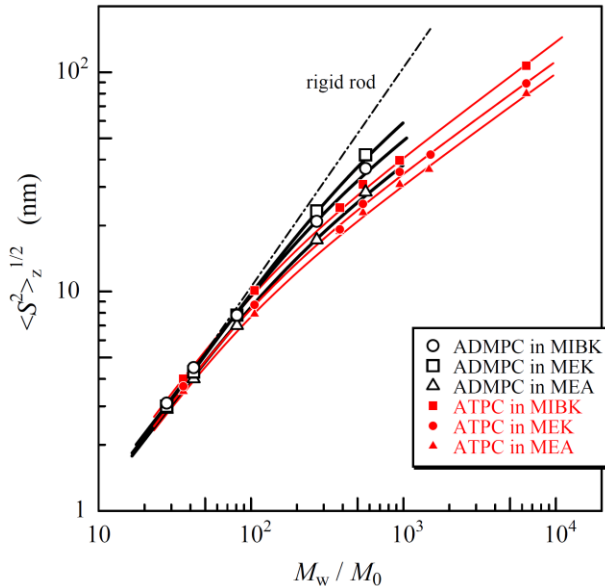

Figure 5. Molecular weight dependence of $<S^2>_z^{1/2}$ for ADMPC in MIBK (open squares), MEK (open circles), and MEA (open triangles) and for ATPC in MEK (filled circles) along with our previous data [11] for ATPC in MEA (filled triangles) and MIBK (filled squares), all at 25 °C. Solid curves, theoretical values for the wormlike chain model with the parameters in Table 2; a dot-dashed curve, theoretical values in the rod limit ($h = 0.37$ nm). See ref [11] for the wormlike chain parameters of ATPC in MIBK and MEA.

Side Group and Solvent Dependence of Chain Stiffness and Local Chain Length. The Kuhn segment length λ^{-1} and the helix pitch per residue h (= M_0/M_L) thus obtained are presented in Table 3 along with the literature values for ATPC in various solvents[11,17] and those for CDMPC[19] and CTPC.[13,20] The latter parameter (h) of ADMPC are in a narrow range between 0.36 and 0.38 nm which are substantially the same as the literature value estimated from the optimized 3D-structures[36] and those for ATPC in MEA, ethyl acetate (EA), and MEK, but slightly smaller than that for ATPC in MIBK (h = 0.42 nm). This possibly suggests that the helical structure of ADMPC is less affectable by the solvent molecules. Substantially the same IR spectra around the NH stretching region for ADMPC17K (Figure 6) support this suggestion.

Table 3. Values of the Helix Pitch per Residue h and the Kuhn Segment Length λ^{-1} for Amylose and Cellulose Phenylcarbamates

Polymer	Solvent	T (°C)	h (nm)	λ^{-1} (nm)
ADMPC	MIBK	25	0.36 ± 0.02	73 ± 5
	MEK	25	0.38 ± 0.02	41 ± 3
	MEA	25	0.36 ± 0.02	22 ± 2
ATPC	MIBK [a]	25	0.42 ± 0.02	24 ± 2
	EA [a]	33	0.39 ± 0.02	17 ± 2
	MEK	25	0.39 ± 0.02	18 ± 2
	MEA [a]	25	0.37 ± 0.02	15 ± 2
	DIOX [b]	25	0.34 ± 0.01	22 ± 2
	2EE [b]	25	0.32 ± 0.01	16 ± 2
CDMPC	NMP [c]	25	0.52	16
CTPC	NMP [d]	25	0.49	16
	THF [e]	25	0.50 ± 0.04	21 ± 2

[a] Ref. [11], [b] ref. [17], [c] ref [19], [d] ref [13], [e] ref [20], DIOX: 1,4-dioxeane, 2EE: 2-ethoxyethanol, THF: tetrahydrofuran.
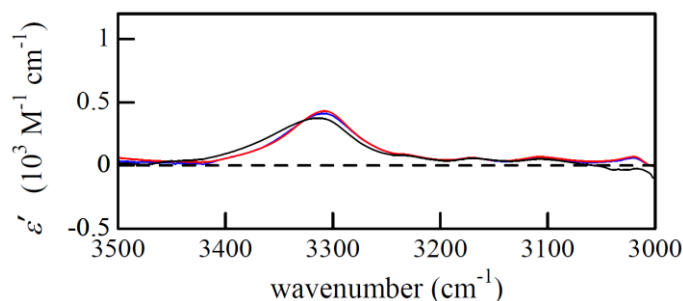

Figure 6. IR spectra (molar absorption coefficient ε' vs wavenumber) for ADMPC17K in MIBK (red), MEK (blue), and MEA (black) at 25 °C.

On the contrary, λ^{-1} of ADMPC in each solvent is appreciably larger than that of ATPC, indicating that the steric hindrance of additional methyl groups appreciably stiffens the amylosic main chain. This is in contrast to the case of cellulosic chains; the wormlike chain parameters of CDMPC are substantially the same as those of CTPC. Furthermore, λ^{-1} of 73 nm for ADMPC in MIBK is the highest value which has been reported for phenylcarbamate derivatives of polysaccharides including mannan (λ^{-1} = 11 nm)[7e] and chitosan (λ^{-1} = 24 nm),[37] and it is comparable to that for a tightly-wounded rigid-helical amylosic chain, that is, amylose tris(n-butylcarbamate) in tetrahydrofuran (λ^{-1} = 75 nm).[38] The value of λ^{-1} increases with increasing molar volume of the solvents v_M (Figure 7); this increment is significantly higher than that for ATPC. Considering polar carbamate groups of ADMPC are preferably located inside[2] and the h value in the three solvents are substantially the same as amylose

9

triesters in the crystalline state,[39] in which there are no significant intramolecular H-bonds, it is not reasonable to suppose that this significant solvent dependence of λ^{-1} is mainly due to the intramolecular H-bonds. Thus, we may suggest that the solvent molecule interacting with the NH groups of ADMPC and ATPC through H-bonding hinders the internal rotation of the main chain and the effect is more significant for ADMPC.
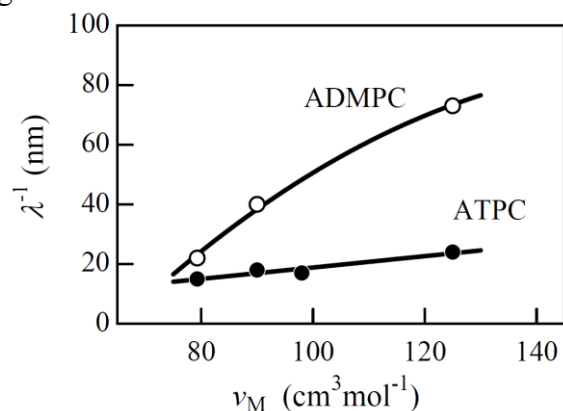

Figure 7. Dependences of λ^{-1} on the molar volume of the solvent (v_M) for ADMPC (open circles) and ATPC (filled circles) in ketones and esters.

Concluding Remarks

Chain stiffness of ADMPC in MEA, MEK, and MIBK is significantly higher than that for ATPC in the corresponding solvent. Although the Kuhn segment length λ^{-1} for ATPC ranges between 16 – 24 nm, λ^{-1} significantly increases with v_M and varies from 22 to 73 nm; the latter value is the highest for phenylcarbamate derivatives of polysaccharides. This significant solvent dependence of λ^{-1} is most likely due to the steric hindrance of the side group and H-bonding solvent molecules. In contrast, their h depends rather insignificantly on the solvents (0.36 – 0.38 nm), while h for ATPC in the same solvents varies in a slightly wider range from 0.37 to 0.42 nm,[11] suggesting that the local helical structure of ADMPC is less sensitive to the solvent.   This difference in the conformational feature between the two amylose carbamates may have something to do with their dissimilar functionality as chiral stationary phase.[16]
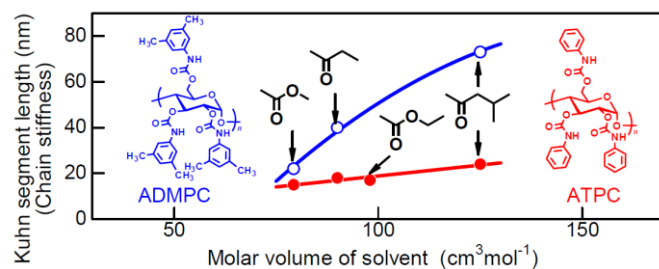
Supporting Information Available: Concentration dependence of $(Kc/R_{0,\mathrm{Uv}})^{1/2}$ and the specific refractive index increments $\partial n/\partial c$ for ADMPC in MIBK, MEK, MEA. This material is available free of charge via the Internet at http://pubs.acs.org.

References and Notes
1. (a) Ikai, K.; Okamoto, Y. *Chem. Rev.* **2009**, *109*, 6077-6101. (b) Okamoto, Y. *J. Polym. Sci. Part A: Polym. Chem.* **2009**, *47*, 1731-1739. (c) Yamamoto, C.; Okamoto, Y. *Bull. Chem. Soc. Jpn.* **2004**, *77*, 227-257.
2. Yamamoto, C.; Yashima, E.; Okamoto, Y. *J. Am. Chem. Soc.* **2002**, *124*, 12583-12589.
3. Kasat, R. B.; Zvinevich, Y.; Hillhouse, H. W.; Thomson, K. T.; Wang, N.-H. L.; Franses, E. I. *J. Phys. Chem. B.* **2006**, *110*, 14114-14122.
4. Wenslow, R. M. Jr.; Wang, T. *Anal. Chem.* **2001**, *73*, 4190-4195.
5. Wang, T.; Wenslow, R. M. Jr. *J. Chromatogr. A.* **2003**, *1015*, 99-110.
6. Ma, S.; Shen, S.; Lee, H.; Yee, N.; Senanayake, C.; Nafie, L. A.; Grinberg, N. *Tetrahedron: Asymmetry* **2008**, *19*, 2111-2114.
7. (a) Burchard, W. *Z. Physik. Chem.* **1964**, *42*, 293-313. (b) Burchard, W. *Makromol. Chem.* **1965**, *88*, 11-28. (c) Banks, W.; Greenwood, C. T.; Sloss, J. *Eur. Polym. J.* **1971**, *7*, 879-888. (d) Burchard, W. *Br. Polym. J.* **1971**, *3*, 214-221. (e) Sutter, W.; Burchard W., *Makromol. Chem.* **1978**, *179*, 1961-1980.

(f) Hsu, B.; McWherter, C. A.; Brant, D. A.; Burchard, W. *Macromolecules* **1982**, *15*, 1350-1357. (g) Pfannemüller, B.; Schmidt, M.; Ziegast, G.; Matsuo, K. *Macromolecules* **1984**, *17*, 710-716. (h) Muroga, Y.; Hayashi, K.; Fukunaga, M.; Kato, T.; Shimizu, S.; Kurita, K. *Biophys. Chem*. **2006**, *121*, 96-104.

8. Kratky, O.; Porod, G. *Recl. Trav. Chim. Pays-Bas* **1949**, *68*, 1106-1122.

9. Yamakawa, H. *Helical Wormlike Chains in Polymer Solutions*; Springer: Berlin, 1997.

10. Yamakawa, H. *Polym. J.* **1999**, *31*, 109-119.

11. Fujii, T.; Terao, K.; Tsuda, M.; Kitamura, S.; Norisuye, T. *Biopolymers* **2009**, *91*, 729-736.

12. Sano, Y.; Terao, K.; Arakawa, S.; Ohtoh, M.; Kitamura, S.; Norisuye, T. submitted to *Polymer*.

13. Norisuye, T.; Tsuboi, A.; Sato, T.; Teramoto, A. *Macromol. Symp.* **1997**, *120*, 65-76.

14. Kitamura, S.; Yunokawa, H.; Mitsuie, S.; Kuge, T. *Polym. J.* **1982**, *14*, 93-99.

15. Waldmann, H.; Gygax, D.; Bednarski, M. D.; Shangraw, W. R.; Whitesides, G. M. *Carbohydr. Res.* **1986**, *157*, c4-c7.

16. Okamoto, Y.; Aburatani, R.; Fujimoto, T.; Hatada, K. *Chem. Lett.* **1987**, 1857-1860.

17. Terao, K.; Fujii, T.; Tsuda, M.; Kitamura, S.; Norisuye, T. *Polym. J.* **2009**, *41*, 201-207.

18. Tsuboi, A.; Yamasaki, M.; Norisuye, T.; Teramoto, A. *Polym. J.* **1995**, *27*, 1219-1229.

19. Tsuboi, A.; Norisuye, T.; Teramoto, A. *Macromolecules* **1996**, *29*, 3597-3602.

20. Kasabo, F.; Kanematsu, T.; Nakagawa, T.; Sato, T.; Teramoto, A. *Macromolecules* **2000**, *33*, 2748-2756.

21. Berry, G. C. *J. Chem. Phys.* **1966**, *44*, 4550-4564.

22. Yamakawa, H. *Modern Theory of Polymer Solutions*; Harper & Row: New York, NY, 1997.

23. Nagai, K. *Polym. J.* **1972**, *3*, 67-83.

24. Norisuye, T.; Yanaki, T.; Fujita, H. *J. Polym. Sci. Polym. Phys. Ed.* **1980**, *18*, 547-558.

25. Holtzer, A. *J. Polym. Sci.* **1955**, *17*, 432-434.

26. Nakamura, Y.; Norisuye, T. *J. Polym. Sci., Part B: Polym. Phys.* **2004**, *42*, 1398-1407.

27. Yamakawa, H.; Fujii, M. *Macromolecules* **1974**, *7*, 128-135.

28. Yamakawa, H.; Yoshizaki, T. *Macromolecules* **1980**, *13*, 633-643.

29. Barrett, A. J. *Macromolecules* **1984**, *17*, 1566-1572.

30. Yamakawa, H.; Stockmayer, W. H. *J. Chem. Phys.* **1972**, *57*, 2843-2854.

31. Shimada, J.; Yamakawa, H. *J. Chem. Phys*. **1986**, *85*, 591-599.

32. Kikuchi, M.; Mihara, T.; Jinbo, Y.; Izumi, Y.; Nagai, K.; Kawaguchi, S. *Polym. J.* **2007**, *39*, 330-341.

33. Sakurai, K.; Ochi, K.; Norisuye, T.; Fujita, H. *Polym. J.* **1984**, *16*, 559-567.

34. Benoit, H.; Doty, P. *J. Phys. Chem.* **1953**, *57*, 958-963.

35. Konishi, T.; Yoshizaki, T.; Saito, T.; Einaga, Y.; Yamakawa, H. *Macromolecules* **1990**, *23*, 290-297.

36. Yamamoto et al.[2] reported that the helical structure of ADMPC optimized by use of the NOESY-NMR results in CDCl$_3$ is similar to that of amylose triisobutyrate (fourfold helix with h = 0.403 nm); similar value h = 0.39 nm was also predicted by Kasat et al.[3] by molecular modeling.

37. Kuse, Y.; Asahina, D.; Nishio, Y. *Biomacromolecules* **2009**, *10*, 166-173.

38. Terao, K.; Murashima, M.; Sano, Y.; Arakawa, S.; Kitamura, S.; Norisuye, T. *Macromolecules*, **2010**, *43*, 1061-1068.

39. (a) Zugenmaier, P.; Steinmeier, H. *Polymer* **1986**, *27*, 1601-1608. (b) Takahashi, Y.; Nishikawa, S. *Macromolecules* **2003**, *36*, 8656-8661.

For Table of Contents Use Only

Solution Properties of Amylose Tris(3,5-dimethylphenylcarbamate) and Amylose Tris(phenylcarbamate): Side Group and Solvent Dependent Chain Stiffness in Methyl Acetate, 2-Butanone, and 4-Methyl-2-pentanone

Maiko Tsuda, Ken Terao,* Yasuko Nakamura, Yusuke Kita, Shinichi Kitamura, and Takahiro Sato